Journal of Materials and Engineering Structures

Experimental and numerical analysis of the fields of the frozen stresses in an epoxy sphere using the method of freezing mechanical cutting

***Kamel Touahir*[a, b, c,*], *Ali Bilek*[a, b], *Philippe Bocher*[c], *Mustapha Beldi*[a, b]**

[a]*L.M.S.E Laboratory, Mechanical Engineering Department, Mouloud Mammeri University Algeria,*

[b]*Mechanical Engineering Department, Mouloud Mammeri University, Algeria,*

[c] *LOPFA, Departement of Mecanical Engineering, Ecole de technologie supérieure. 1100Rue Notre-Dame Ouest, Montreal, H3C 1K3, Canada,*

ARTICLE INFO

Article history :

Received 00 December 00

Received in revised form 00 January 00

Accepted 00 February 00

Keywords:

Contact

Isoclinic

Isochromatic

Stress

Photoelasticity

ABSTRACT

The stresses induced by a mechanical contact imposed on a birefringent sphere have been studied experimentally and numerically. The birefringent sphere is machined from a birefringent parallelepiped on a high speed numerically controlled machine. The residual stresses developed in the birefringent sphere have been eliminated by a thrmic treatment of relaxation. The technique of freezing and mechanical cutting in thin slices was used. In the case of 3D photoelasticity, the frozen stress techniques, which are very much used, may introduce residual stresses in the cut up slices. Although the means to avoid the introduction of these residual stresses are well established, these techniques remain time consuming. Slices are analyzed on a polariscope using plane light and circular light. The photoelastic fringes are used to determine the principal directions of the stresses as well as the values of the stresses. A numerical simulation using the finite elements made it possible to make a comparison with the experimental results. The analysis shows a good correlation between experimental measurements and numerical simulation.

NOMENCLATURE

a	Amplitude of the light wave [nm]
n_1	Refractive index along the direction of σ_{max}
n_2	Refractive index along the direction of σ_{min}
f	Isochromatic fringe value [N.mm]

* *Corresponding author. Tel.: +213 5 53 96 39 87.*
E-mail address: touahirkamel@yahoo.fr

e-ISSN: 2170-127X,

RESEARCH REVIEW of Sciences and Technologies

α	Isoclinic parameter [degree (°)]
φ	Isochromatic parameter [degree (°)]
λ	Light wave length used for the experiment [nm]
F	Normal load [N]
δ	Relative retardation [nm]
e	Model thickness [mm]
N	Fringe order
μ_1	Poisson's ratio of the birefringent model
μ_2	Poisson's ratio of the metal cylinder

1. Introduction

In mechanical systems several parts can come into contact, thus transmitting motion and power. Knowledge of the deformations in the vicinity of the contact zones can help predict the service behavior of the parts. Several methods can be used to measure deformations. We will use here the photoelasticimetry which is an interesting method because it allows having a complete field of stresses. Several studies have been conducted [1; 3-6; 8-18] experimentally and numerically to analyze and study contact problems. The stresses are generally concentrated in the vicinity of the contact zone and decrease very quickly while moving away from this zone. The method consists on freezing stresses in the volume of the model by using the properties of the molecular chains of certain polymers (epoxy, polycarbonate ... Etc.). When the model is loaded in the highly elastic state, then cooled slowly to room temperature, it retains almost all the acquired birefringence in the highly elastic state. This stress freezing technique is based on the biphasic behavior of some materials when heated to a critical temperature. These polymers are composed of two types of chains connecting the molecules to each other: the main chains and the secondary chains. At room temperature both types of chains resist the loads applied to the model. When the temperature of the polymer increases to the glass transition temperature (about 130 ° C for the epoxy), the secondary chains give way and therefore only the main chains then support stresses. The charge being maintained, slowly decreasing the temperature of the polymer to room temperature, the secondary chains are reformed between the strongly deformed main chains. When the load is removed, main strings relax slightly, but a considerable proportion of the deformation is preserved. The elastic deformations of the main chains are then fixed in the volume of the model permanently thanks to the reformed secondary chains [9]. This property is used to study stresses in three-dimensional parts. Once the model has cooled down and the stresses are frozen, it is cut into thin slices so that the stresses are relatively identical through the thickness. If possible, the slices are cut according to particular plans, such as planes of symmetries, meridian plans ... etc. They are studied by a two-dimensional photoelasticimetry method, without forgetting to consider the normal stress on their plans as non-zero. These normal stresses are obtained from other sections, for example, perpendicular to the previous ones, or cutting the slice into "slices", to be able to observe it in perpendicular directions. The analysis of the fringe pattern is carried out manually by point measurement; this requires a lot of time. With the development of computer science and image acquisition and processing techniques, several methods have been developed [10-11; 2]. J.C. Dupré and A. Lagarde [2] have developed a method for 3D visualization of isochromatic and isoclinic fringes developed in transparent (epoxy) solids in contact using the light scattering phenomenon and the superposition properties of these light fields. The model to be analyzed is cut optically using two laser beams. They were able to analyze the field of the stress in all the volume of the solids in contact. A parallelepiped loaded by a force centered in the middle was used. A. Zénina [4-5] has developed a method of 3D visualization of a torsion test on a prismatic bar (epoxy) using the optical cutting method using a monochromatic CCD camera. This optical slicing requires only a few seconds to get the results.

Budimir [6] presented a numerical procedure for the two-dimensional elastic problem. In his Hertz contact model between two solids, considering the state of constraint plane, he showed a good correlation with the theoretical results. Contact stresses were calculated using materials with different elastic modulus: an aluminium cylinder on a rectangular steel plate. He showed that the maximum normal stress is at the center of the contact surface and invariably decreases to zero at the end. As a result, the contact surfaces are a function of the Young's module of the two solids in contact. He also studied the effect of friction with the same pair of materials. He also analyzes the adhesion and slip conditions for different Young's modulus materials. L. kogut [12] presented in his work a finite element analysis of an elastic contact of a deformable sphere

compressed by a rigid parallelepiped. The plastic elastic contact of a sphere on a plane is of fundamental importance in contact mechanic. It finds its application in the study of wear problems, of friction and also in the thermal and electrical conductivity between rough contact surfaces. Kogut uses the VON MISES criterion to detect the local transition between elastic and plastic deformations. He showed an evolution of the elastic contact with three stages that go from the purely elastic contact to the plastic elastic contact and finally to the purely plastic contact.

A. Bilek [13] used a non-destructive optical slicing method for the case of a rigid aluminum cylinder in contact with an epoxy deformable parallelepiped at room temperature. A rigid aluminum parallelepiped is in contact with a deformable epoxy cylinder at freezing temperature (120 °) and a rigid aluminum cylinder on a cylindrical deformable epoxy model, inside an oven. The basic idea is to use the polarization properties of scattered light by studying thin slices of the model.

In this study, we used two methods, experimental analysis using photoelasticity and numerical analysis. In the experimental part, a mechanical device made it possible to freeze the stress. A sphere made of deformable birefringent material (epoxy) is stressed in compression thanks to a rigid steel cylinder.

The initial residual stresses were eliminated by a relaxation heat treatment. The stresses are fixed in the model inside an oven using a heat treatment. After cooling, the model is cut into several thin slices. The most sought-after slice has been studied and compared with the finite elements using the CASTEM software.

2. Experimental Procedure

2.1.1 Elimination of residual stresses

Residual stresses are stresses that modify the mechanical properties of materials such as hardness and resilience. For metals (steel, aluminum, cast iron...etc.), the stress are due to the orientation of the planes (disturbance of the crystal lattice). It is not an easy task for researchers and designers to eliminate residual stresses. Before analyzing models, specimens and samples, it is necessary to check the presence of the residual stresses. As for transparent materials, they can be observed using a polariscope, but what about metals; we can not observe the residual stresses even if we did thermal treatments annealing). There will always be questions to ask (Fig. 1). Several results were found approximately, researchers are not yet able to find methods that can validate their results in optical methods. There are several stresses such as mechanical stresses, thermal stresses, chemical stresses ... etc; these are stresses that must be validated by experimental, numerical and analytical methods.

In aerospace, such a method is of particular interest since it is used to observe the stresses and to obtain components in the materials, epoxy, used here, is a thermoplastic resin (TD) polymer material having an amorphous structure with a glass transition temperature T_g of about 120 ° C. It is a macromolecule based on carbon, formed by the crosslinking of several monomers $\left(CH_2 - O - CH\right)_n$; the residual stresses are due to the structure of the resin (TD) and the rise in temperature which is of the order of T_g . In this case the residual stresses visualized under the polariscope (Fig. 1) are due to the machining.

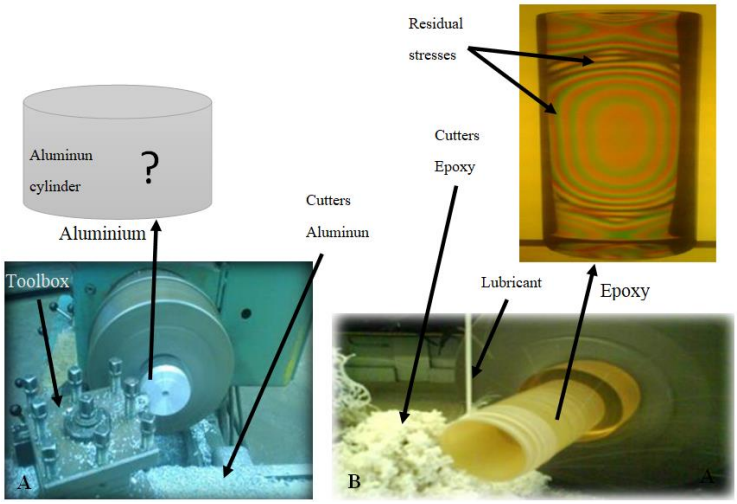

Fig. 1- Machining of the aluminium cylinder (A) and of the epoxy cylinder (B)

Visualization of residual stresses for a cylinder in 3D

The model must be introduced into the oven. The temperature is then increased to 120 ° C at 5 ° C per hour (Fig. 2). The model remains in the oven for 3 to 12 hours depending on the volume of the room for homogenization of the temperature. The model is then cool before being removed from the oven. The cooling temperature of a model with variable sections is determined by the largest thickness of the variable sections and determined by the largest thickness of the part. A table provided by the manufacturer of the PLM-4R allows to choose the cooling rate according to the thickness of the model.

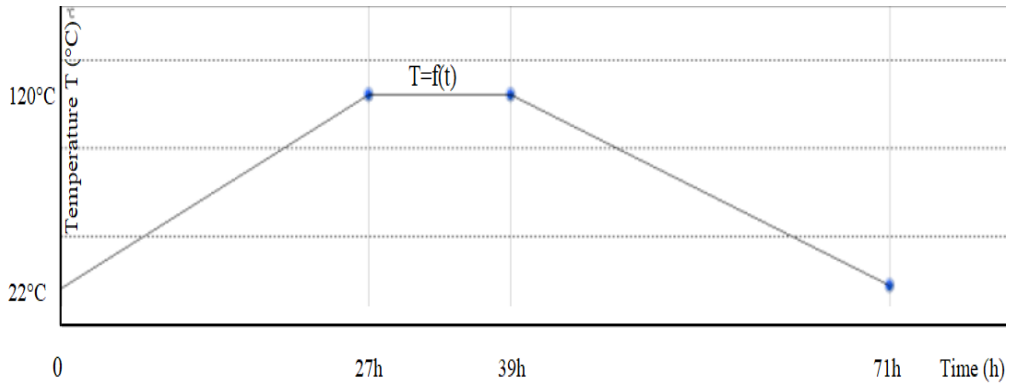

Fig. 2- Thermal cycle for annealing

The model is then ready to be used, such as, at room temperature or undergo the stress freezing process when using the stress freezing method or the three-dimensional photoelasticimetric optical slicing method for determining the stresses in the model volume (Fig. 3).

Fig. 3- Visualizations of the model under the polariscope after elimination of the residual stresses for an epoxy cylinder

2.1.2 Experimental apparatus

The experimental setup consists of a loading device. The model is mounted in the loading device. A steel model is used to apply a compressive load on a deformable model. The results are retrieved from the polariscope after displaying the stress and mechanical cutting, as an image, using a digital camera. The isochromatics and isoclines obtained make it possible to analyze the stress field.

A rigid steel cylinder 30 mm in diameter and 20 mm thick is used to apply a compression load of 150N on a deformable sphere (Fig. 4). The axes of both models are orthogonal. The stresses were fixed inside the volume of the sphere using the stress freezing method. The sphere is then cut into thin slices for further analysis on a polariscope.

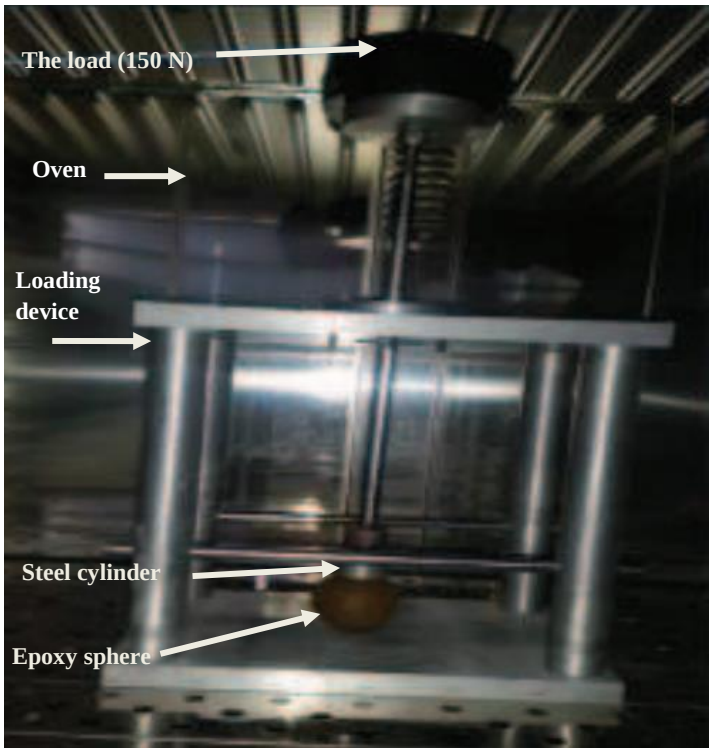

Fig. 4- Detailed view of the experimental setup

The birefringence phenomenon is used here to analyze the stress fields. Figure 5 shows the well known photoelastic method based on the birefringent phenomenon [11] of some transparent materials.

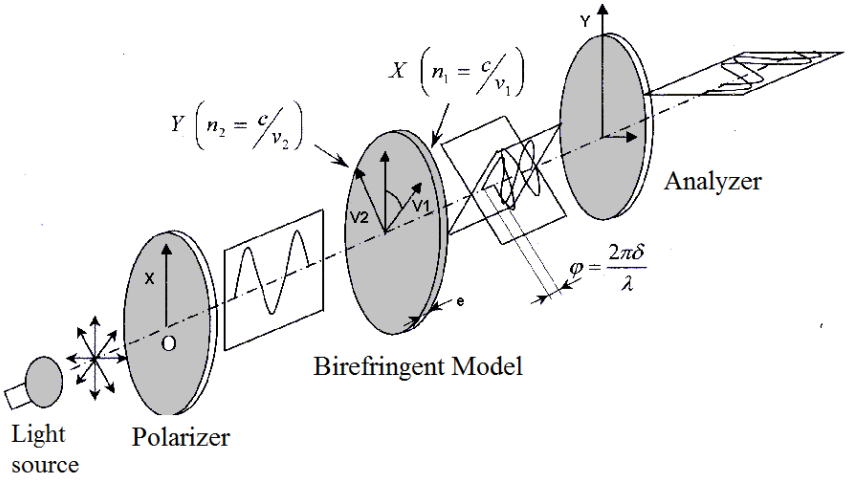

Fig. 5- Light propagation through a photoelastic model.

The light intensity obtained on the analyzer (Fig. 5) is given by the following relation (equation 1) [1].

$$I = a^2 \sin^2 2\alpha \sin^2 \varphi/2 \tag{1}$$

The terms $sin^2 2 \propto$ and $sin^2 \varphi/2$ give, respectively, the principal stresses directions and the values of their difference with the following relation (equation 2):

$$\sigma_1 - \sigma_2 = \frac{N\ f}{e} \tag{2}$$

Where N is the fringe order obtained experimentally from the isochromatic fringe pattern, e is the slice thickness and f is the fringe constant which depends on the light wavelength λ used and the optical constant C of the model material (f= λ/C). The value of the fringe constant f is determined experimentally with a disc of the same material as the model. The disc, introduced in the oven with the model, is loaded along the diameter. After cooling the disc is analyzed with the circularly polarized light in order to obtain the fringe constant which is used then to obtain stresses [1; 22; 23]. The value obtained is f = 0.36N/mm/fringe [23].

2.2 Experimental Results

2.2.1 The isochromatic fringes

We analyzed a slice of relatively large thickness (10mm) so as to obtain several fringes. To obtain the experimental fringes, it was necessary to use a zoom. We distinguish the fringes and we notice that their number increases when approaching the contact zone. They then decrease to cancel themselves away from the contact zone. The fringes obtained are shown on (Fig. 6).

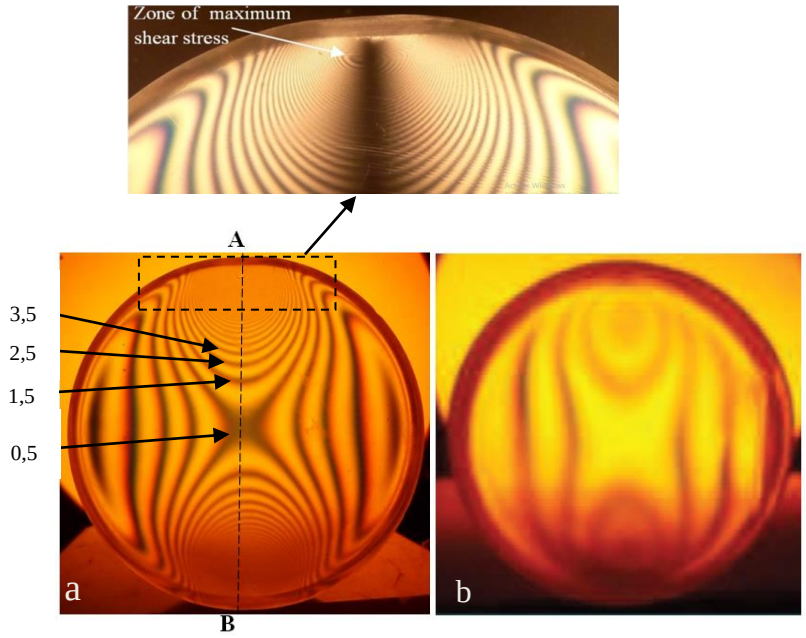

Fig. 6- Experimental isochromatic fringes at z=0 mm (slice a) and at z=10 mm (slice b).

It can be seen that the stresses are localized to the neighborhoods of the contact zone; it is also observed that the stresses developed in the different slices diminish as they move away from the direction of application of the load. On both sides of contact of the sphere, it is therefore far from the point of application of the load there is no fringes. The stresses are negligible (Fig. 6-A). We note that the closer we get to the line of action of the load, the more the fringes appear (Fig. 6).

The values of the constancy of fringe and Young modulus at freezing temperature used in the numerical calculation were determined using the marker tracking method [21-22; 23] described: f_f =0.36 N/mm/frange, $E_f = 15{,}9\ N/mm^2$.

Figure 7 illustrates the maximum shear stress along the segment [AB]. At each order of bangs, the order of N corresponds to a value of the maximum shear stress given in absolute value. The variation of the maximum shear stress along the [AB] axis is given in the fig. 6, it is found that the stress in the middle of the contact zone takes the value of 0.018 MPa at a distance of 35mm, and then gradually increases to the area of load application. We note that the shear stress τ_{max} takes a maximum value at the point of Hertz and decreases as we move away from this point and this confirms the results obtained by other investigators [14], even the theory of Hertz.

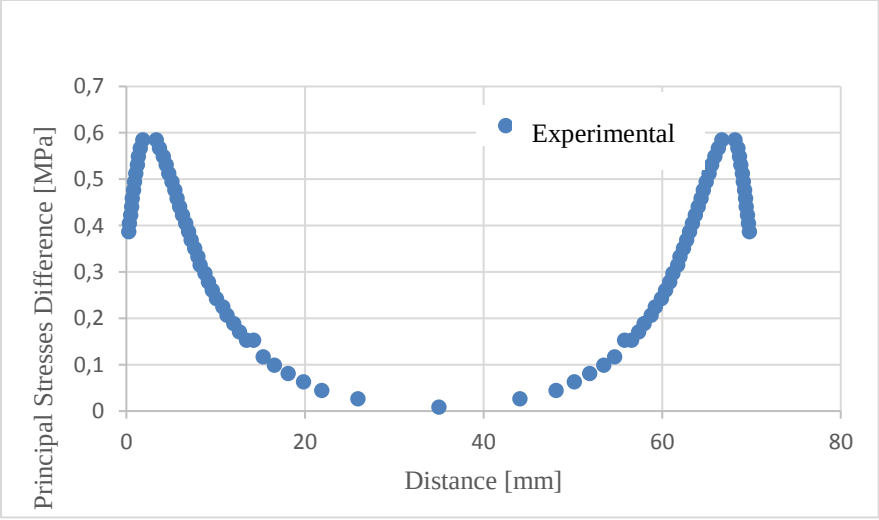

Fig. 7- Experimental values of principal stress difference along the vertical axis of symmetry.

2.2.2 The isoclinic Fringes

By rotating the two Polaroids simultaneously one visualizes the isoclines (Figure 8) that appear one by one according to the angle of rotation. We notice that by turning the two Polaroid, the isocline fringes appear in very visible dark areas in the images and change their position depending on the angle of rotation. It is recalled that the isoclines do not depend on the intensity of the loading; therefore the study on isoclines will be done for a single case of loading.

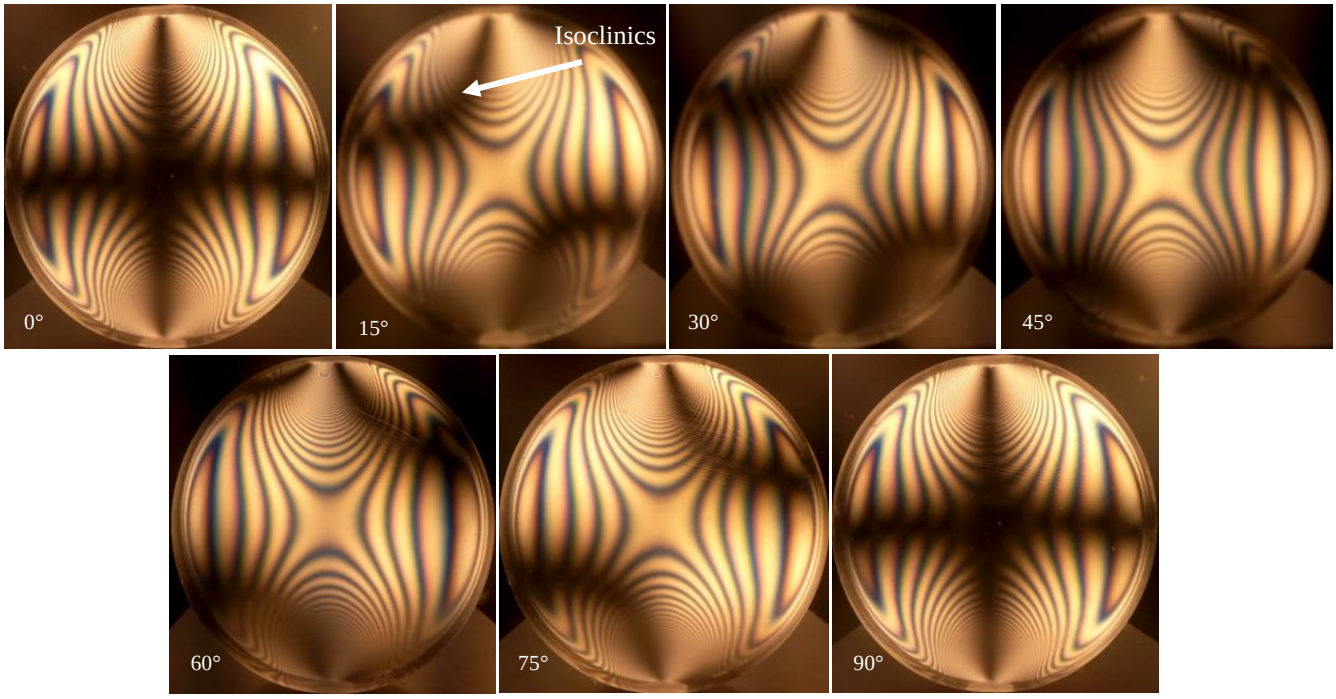

Fig. 8- Isoclinic fringe patterns for two different positions of the polarizer and the analyzer axes (0°,15°, 30°, 45°, 60°, 75° and 90°).

The exploitation of the isoclines makes it possible to determine the principal stresses directions. The principal stresses trajectories called isostatics can be traced from the knowledge of the isoclines. Figure 9 shows the isoclines and isostatics for the case of the sphere identified experimentally and traced manually.

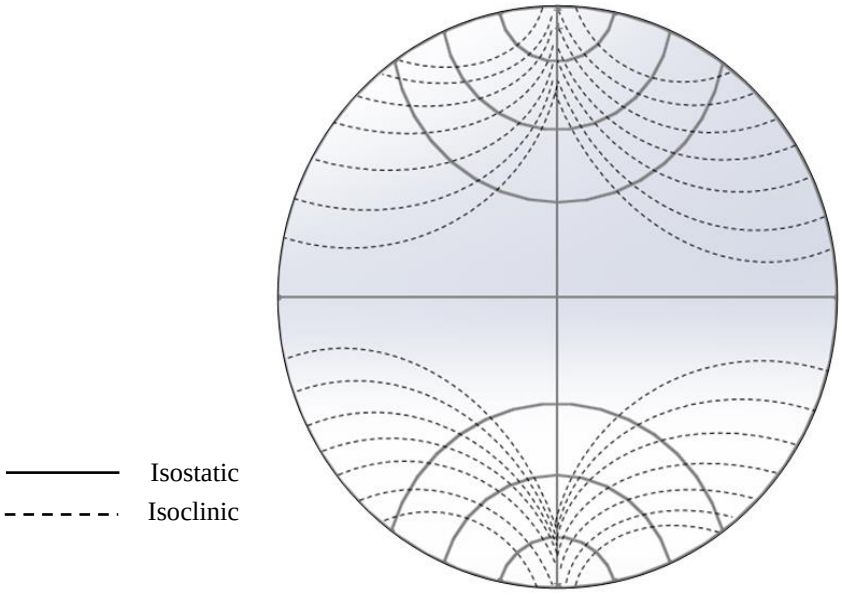

Fig. 9- Isoclinic and isostatic for plane-to-sphere contact

3. Finite Elements Analysis

A finite element analysis conducted with *CASTEM* software. Young's modulus and Poison's ratio for the two bodies in contact are introduced in the program. The isochromatic fringes, the isoclinic fringes and the stress values are determined numerically in order to compare them with the experimental ones. However, we have to determine correctly the optical parameters. The experimental results are obtained for a value of the slice thickness relatively large in order to observe several fringes. Stresses are, therefore, not constant along the thickness of the isolated slice. In the finite element solution, the thick slice is divided into n thin slices to have a better simulation of the applied stresses [7,11]. Every thin slice is then characterized by αi and ϕi, respectively the isoclinic and the isochromatic parameters, constant along its thickness. The meshing of the model (Fig. 10) is refined in the contact zone in order to obtain more accurate results.

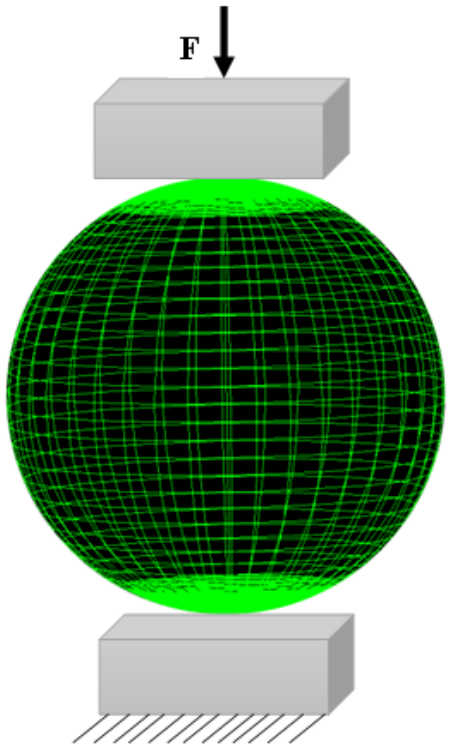

Fig. 10 - Model meshing.

3.1 Application of the Load

In the finite elements solution, we used the vertical displacement of the upper cylinder as this is a more realistic way of applying the load; for each node we calculated the resulting vertical displacement according to its position in the contact zone. The equivalent applied load is obtained, then, as the sum of the elementary vertical loads at the nodes in contact. The iterative process in the incrementing of the vertical displacement stops when the sum of the elementary loads reaches the value of the load (F=150N) set for the experiment. The material is considered to behave everywhere as a purely elastic isotropic material. Fringe constant f=0.36N/mm, Young's modulus (E1=210000 MPa, E2=15.9 MPa) and Poisson's ratios ($\mu 1$=0.3, $\mu 2$=0.45) respectively for the parallelepiped and the sphere are introduced in the finite element program. The mesh is refined in the neighbourhood of the contact zone (Fig. 10) in order to achieve better approximation of stresses.

3.2 Calculating the Isochromatics

The following relation (3)which can be obtained readily from Mohr's circle for stresses allows us to calculate the principal stresses difference at any point of a stressed model.

$$\sqrt{(\sigma_x - \sigma_y)^2 + 4\tau_{xy}^2} = \sigma_1 - \sigma_2 = Nf/e \tag{3}$$

The different values of the retardation angle φ can be calculated at any point on the model using the following relation (4)

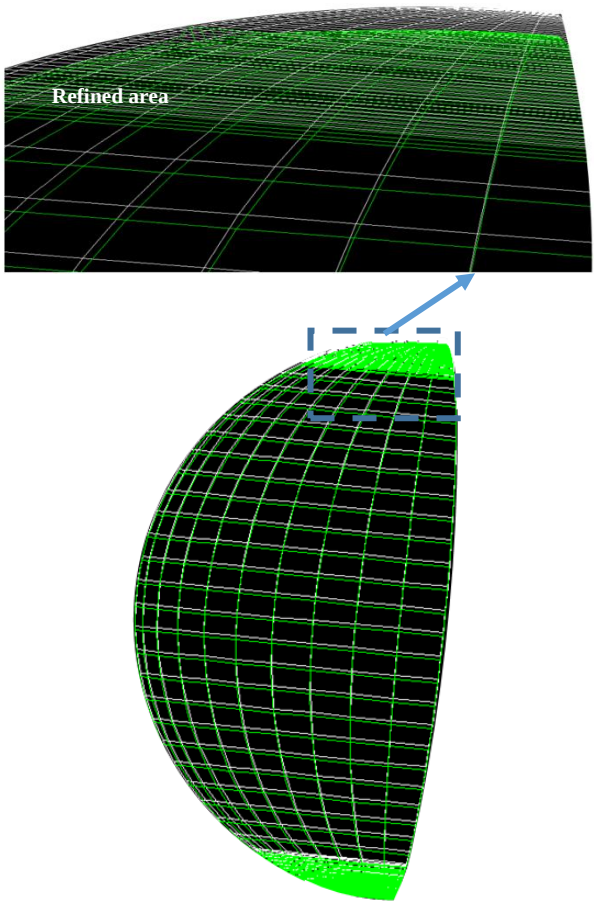

Fig. 11 -.Representation of the Deformed Sphere

$$\varphi = 2\pi N = 2\pi\ e/f \sqrt{(\sigma_x - \sigma_y)^2 + 4\tau_{xy}^2} \tag{4}$$

The different values of $sin^2\varphi/2$ which represents the simulated isochromatic fringes (fig. 12) have been easily calculated. Isochromatics and isoclines (Fig. 12), calculated for each slice using a program written under CASTEM, clearly show that in the upper and lower part of the sphere, away from the load application area, the stress are null (total absences of fringes). They then increase to a maximum value at the point of application of the load (the number of fringes visible is maximum at this location). CASTEM uses a color scale to represent the Isochromatics and isoclines fringes. If for example the light intensity is zero, CASTEM represents it in blue. If the light intensity is maximum, CASTEM represents it in red. CASTEM has four colors: blue, green, yellow and red. The intensity of light is variable between 0 and 1.

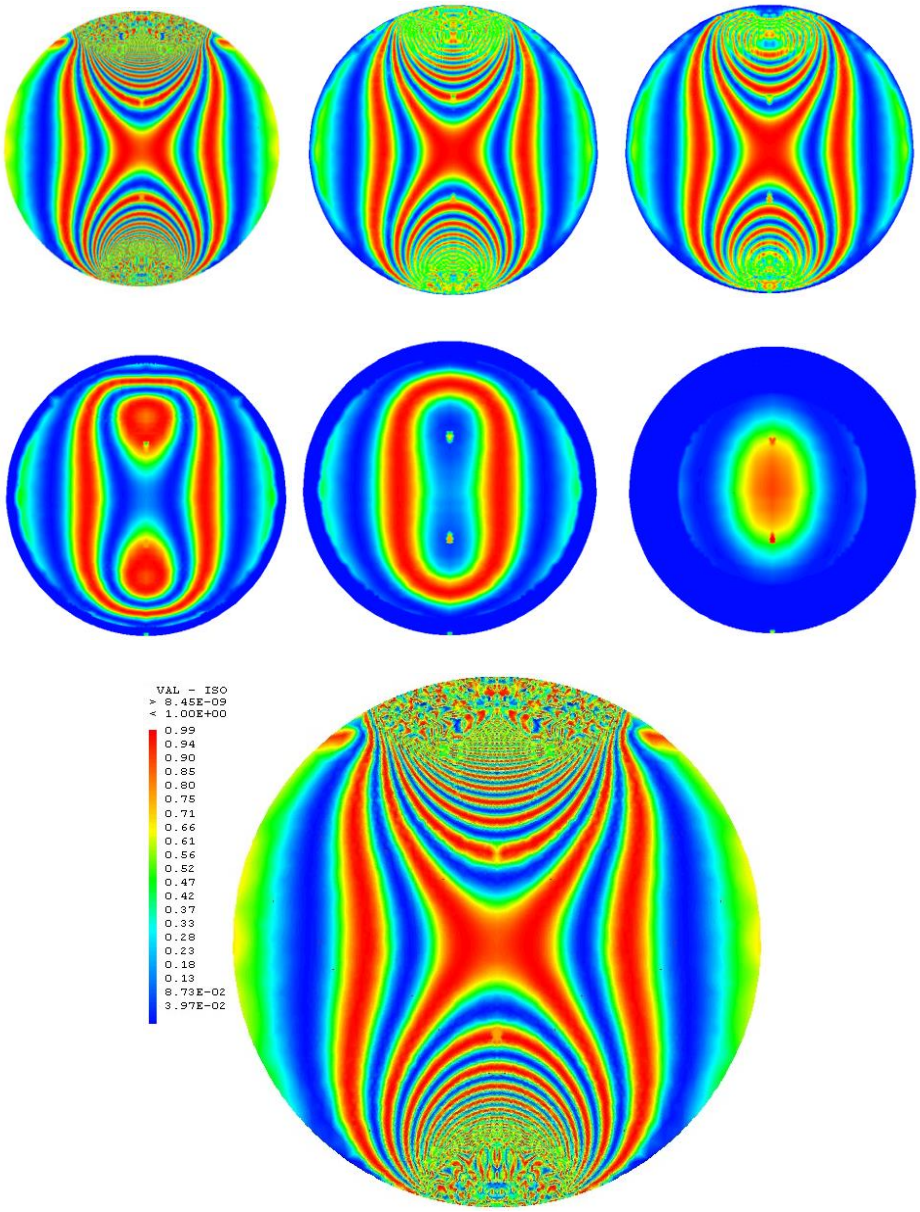

Fig. 12 -.Fringes obtained by finite elements along the sphere by isolating a slice of thickness 8 mm

Images obtained using CASTEM are processed using Photoshop software to obtain black and white fringes (fig.13). To compare the numerical and experimental results, as for the experimental case, the calculations were made with 7 mm thick slice. The fringes thus obtained correspond to the stresses developed in the isolated slice along the axis of the sphere. They are comparable to experimental fringes (fig. 6).

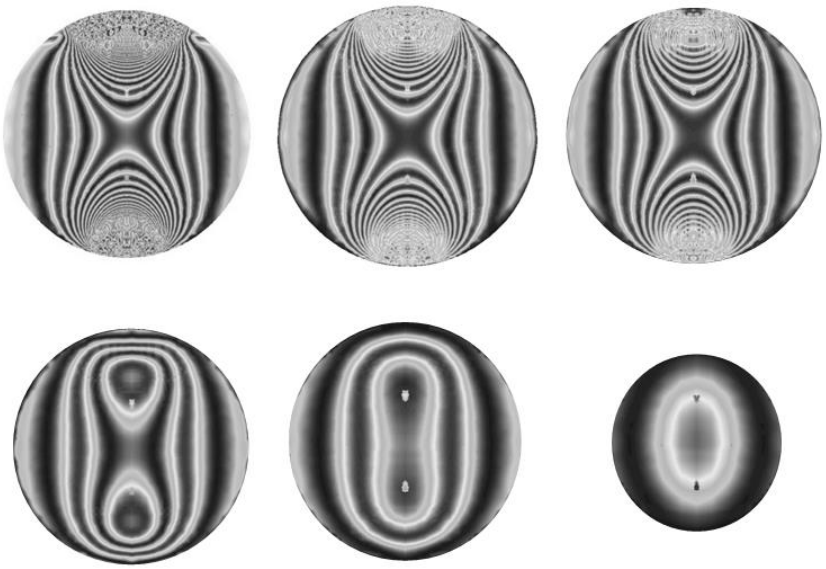

Fig. 13 -.Isochromatic fringes measured by finite elements and treated with Photoshop software

The graph (Fig.14) clearly shows the evolution of the difference in principal stresses along a vertical line along the direction of the applied load.

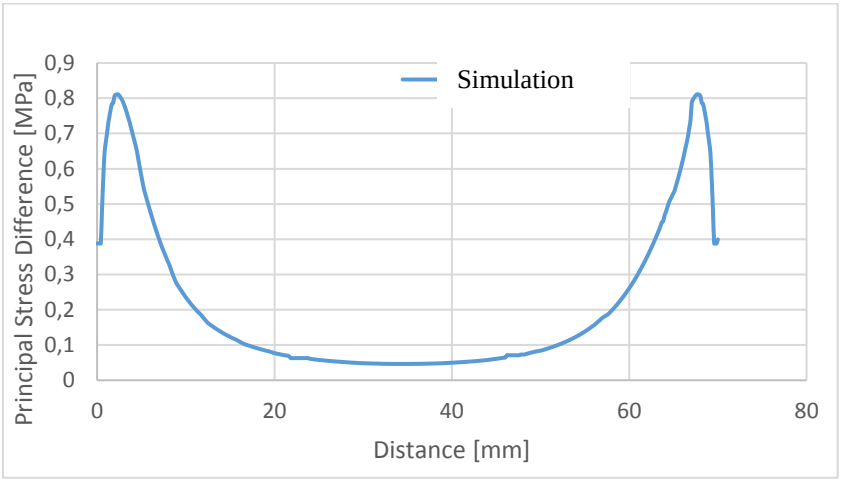

Fig. 14 -.Evolution of the difference of the principal stresses to a segment located along the direction of the load

The difference in the principal stresses increases by approximately 0, 84 MPa to a value of about 0, 39 MPa at a distance of 3, 33 mm. It gradually decreases to a value of 0.018 MPa at 35 mm and then it increases to reach a value of 0.84MPa at a distance 68 mm.

3.3 Calculating the Isoclinic fringes

In the finite elements program the isoclinic fringes are numerically calculated with relation (4) given here after. Isoclinic fringe patterns are obtained for two different settings of the polarizer and the analyzer axis *($\propto$= 0°,15°, 30°, 45°, 60°, 75° and 90°).* The term $sin^2 2 \propto$ represents the isoclinic fringes which are loci of points where the principal stresses

directions are parallel to the polarizer and the analyzer axis. In the simulation program the different values of the isoclinic parameter α can be calculated with the following relation (eq. 4) which can be obtained readily from Mohr's circle of stresses:

$$\alpha = \tan^{-1}\left(2\tau_{xy} / \left(\sigma_x - \sigma_y\right)\right) \tag{4}$$

The different values of $sin^2 2 \propto$ can therefore be calculated and displayed (fig.15).

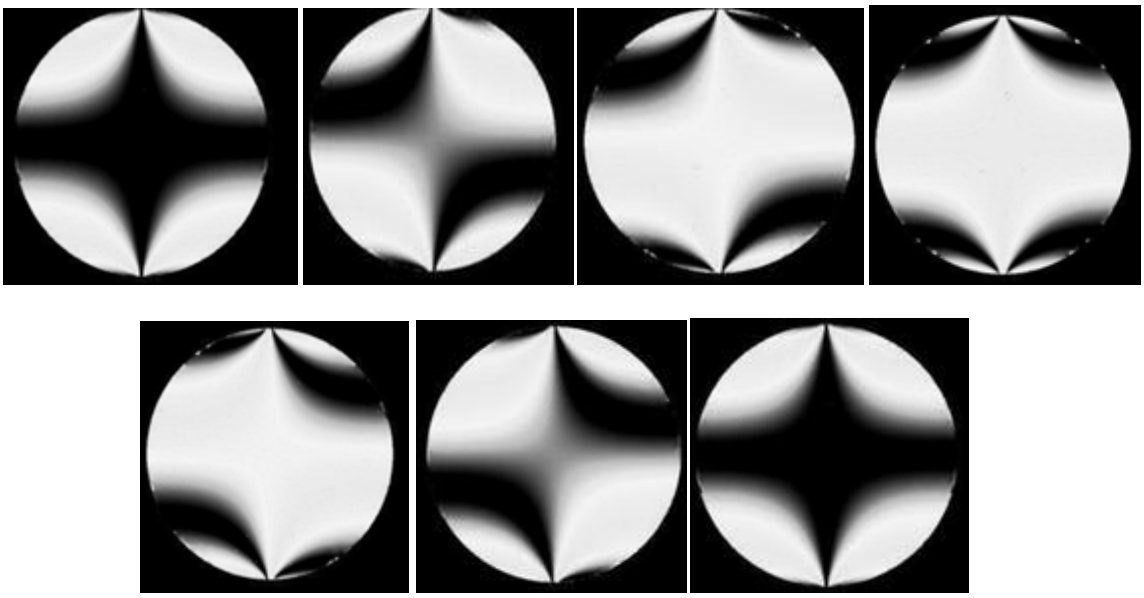

Fig. 15- Calculated isoclinic fringe pattern for 0°,15°, 30°, 45°, 60°, 75° and 90°.

4. Comparison of results

The purpose of this comparison is to validate the results finite elements by the experimental. Two comparisons are possible. The first will be made between the images of the isochrones and isoclines recorded experimentally and those simulated numerically; the second comparison will be made between the curves of the variation of the differences of the principal stresses difference.

4.1 Comparison of isochromatics

Figure 16 shows the experimentally recorded isochromatics and calculated isochromatics with CASTEM and processed with Photoshop.

a) b)

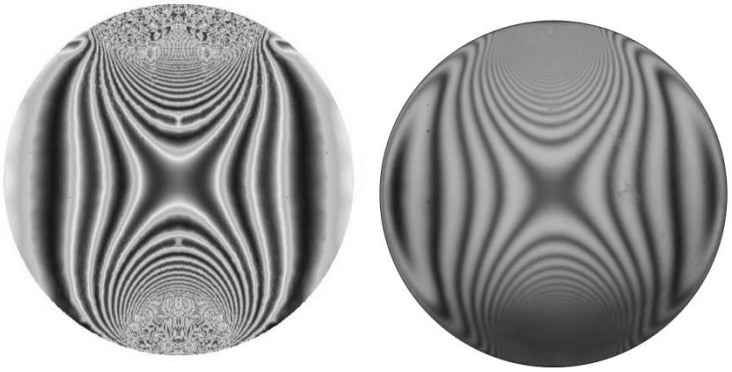

Fig. 16- Isochromatic fringes, simulated (a) and experimental (b).

The simulated fringes are comparable to the experimental fringes in the lower and upper parts of the model. Far from the contact zone, the stress decreases. We note that the experimental image obtained by photoelasticimetry is superimposed largely with the image given by CASTEM and treated with the Photoshop software.

4.2 Comparison of isoclines

For the comparison of the isoclines obtained numerically and experimentally for the different rotations of the angle, the dark part of each image corresponds to the isoclines, area where one of the main directions is parallel to one of the polaroids axes. Fig. 17 represents the superposition of the isoclines obtained numerically and processed with the PHOTOSHOP software (to the left of each image) with the corresponding isoclines obtained experimentally (to the right of each image). Note that it is impossible to separate the isochromic network from the isoclinic network in the images obtained experimentally. Note that the isoclines on the left and right sides of each image are similar and consistent.

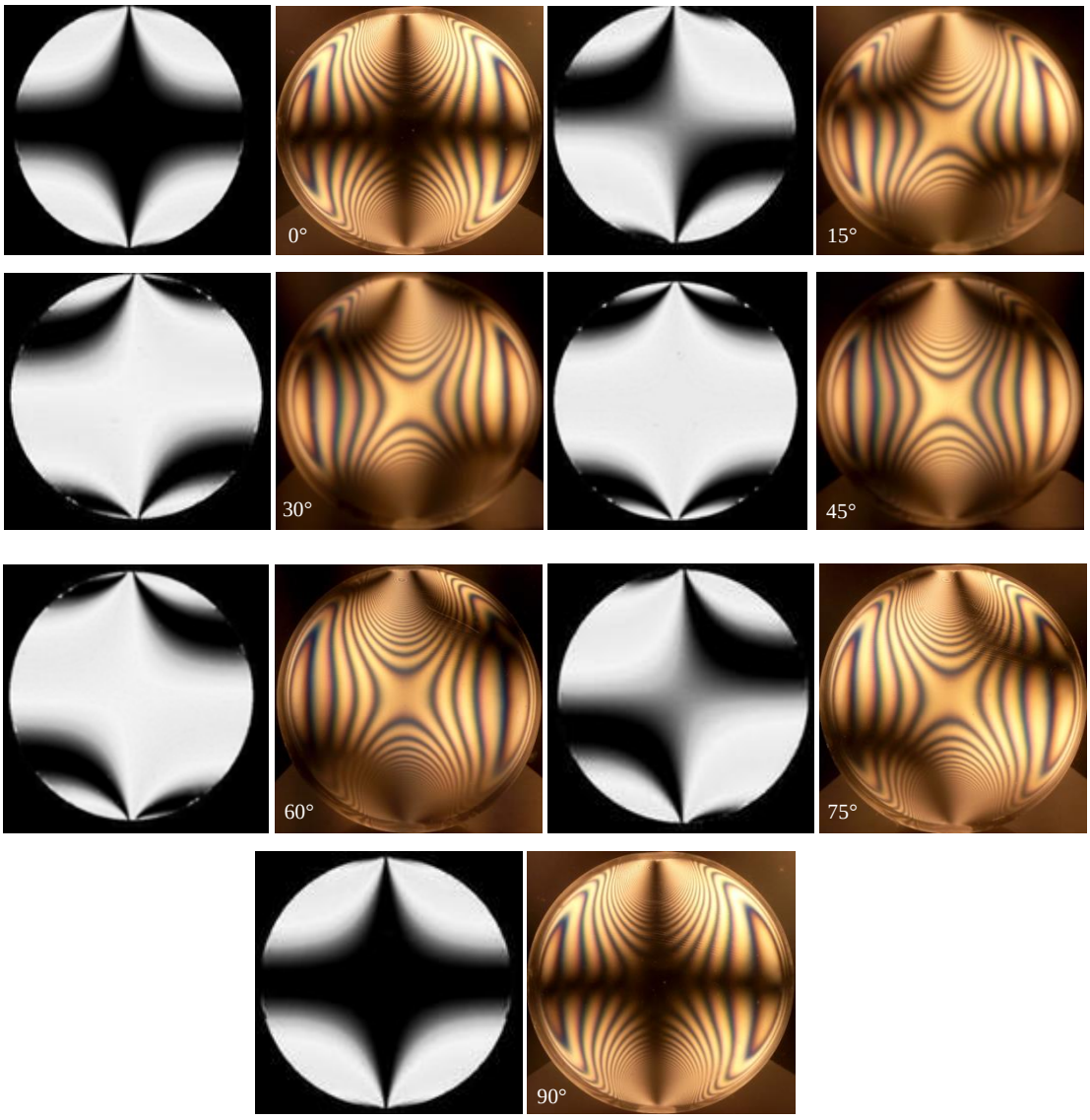

Fig. 17- Comparison of the digital isoclinic fringe pattern and the experimental isoclinic fringe pattern

4.3 Graphs of the principal stresses difference for a slice isolated along the load direction

Figure 18 represents the graphs of the experimental and numerical results. The graph of the difference of the principal stresses along the line [AB] shows, relatively, good agreement between numerical results and experimental results.

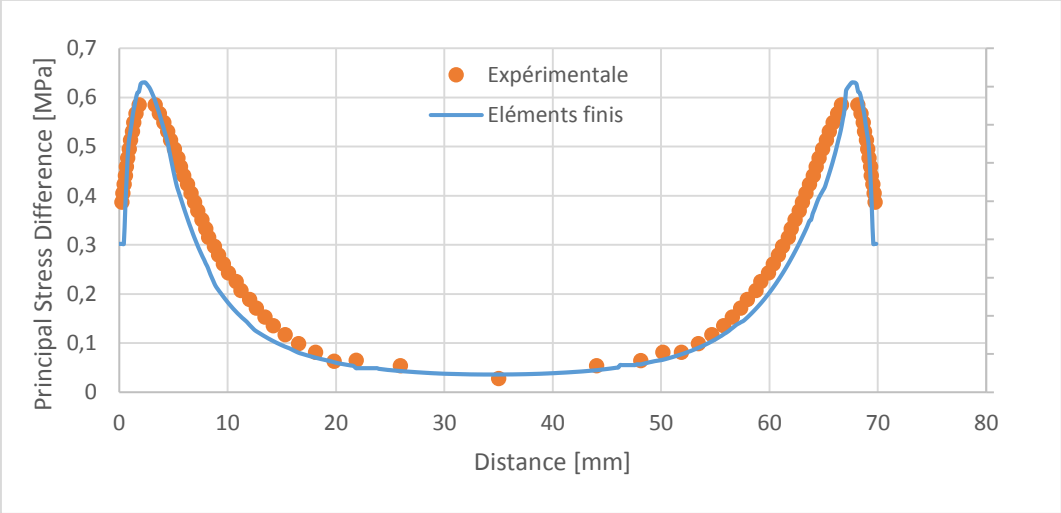

Fig. 18- Principal stresses difference along the vertical axis of symmetry

Using numerical computation it is possible to determine the values of the stress in all the sections of the studied model. However, this is not the case for experimental analysis using photoelasticimetry, it is sometimes difficult to obtain the fringe order and therefore the stresses in the immediate vicinity of the contact zone.

Several authors, Karl-Hans Laermann [19] and D.K. Tamraker [20], have found that many sources of errors could affect the accuracy of digital photoelasticity measurements. Three main reasons can explain the errors observed in our case:

a) For finite element analysis, the behavior of the model is considered to be purely elastic and ignores localized plastic deformations due to stress concentrations in the contact zone. The stress field is therefore no longer the same as that obtained for the purely elastic isotropic case. The zone of plasticization normally decreases the intensity of the stresses and thus the fact of considering a purely elastic isotropic behavior in the zone of contact induces stresses greater than they are actually

b) The type meshing used in the finite element calculation process especially in the contact zone.

c) The accuracy of the experimental measurements, mainly the evaluation of the fringe order which is more difficult and less precise in the vicinity of the contact zone.

5. Conclusion

In this work we have shown that the stress freezing and mechanical slicing method can be successfully used to analyze stress fields developed in the neighbourhood of the contact zones. This technique allows a complete study of a model; Isochromatics as well as isoclinics can be determined experimentally, particularly in the more stressed regions of the models. A finite elements analysis with castem package can give relatively accurate results as long as the limit conditions and the application of the load are correctly simulated.

We have analysed a stress field developed in a birefringent sphere. The purpose is to develop a finite element solution and analyse completely the stress field, particularly in the neighbourhood of the contact zone. We showed that photoelastic fringes and stresses can be calculated easily and accurately for any isolated slice with sufficient accuracy. Good agreements between experimental and numerical results are achieved.

REFERENCES

[1]- J. W Dally and F. W. Riley, Experimental stress analysis, McGraw-Hill, Inc, 1991. Bookmark: https://trove.nla.gov.au/version/30059478

[2]- J.C. Dupré and A.Lagaede, photoelastic Analysis of a three Dimensional Specimen by Optical Slicing and Digital image Processing, Experimental Mechanics Vol.37,No.4, December 1997,pp.393-397. Dupré J.C. & Lagaede, A. Experimental Mechanics (1997) 37:393. https://doi.org/10.1007/BF02317303

[3]- Patterson E. A., J. W. and Wang Z.F., On Image Analysis for Birefringence Measurrement in Photoelasticity, Opt. Lasers Eng., 1997, 28 (1) 17-36. https://doi.org/10.1016/S0143-8166(96)00060-7

[4]- Zénina, A., Dupré, J.C., Lagarde, A., Optical approaches of a photoelastic medium for theoretical and experimental study of the stresses in a three-dimensional specimen , In IUTAM Symposium on Advanced Optical Methods and Applications in Solid Mechanics, A. Lagarde (Ed.) Poitiers (France), p. 49-56, Kluwer Academic Publishers, 1998. DOI 10.1007/0-306-46948-0

[5]- A. Zenina, J.C. Dupré & A. Lagarde, Separation of isochromatic and isoclinic patterns of a slice optically isolated in a 3-D photoelastic medium, Eur. J. Mech. A/Solids 18, pp. 633-640, 1999. https://doi.org/10.1016/S0997-7538(99)00105-9

[6]- Mijović, Budimir, Dzoclo, Mustapha, Numerical contact of a Hertz contact between two elastic solids, Engineering Modeling, 13 (2000), 3-4; 111-117

[7]- A. Mihailidis, V. Bakolas, & N. Drivakovs, Subsurface stress field of a dry line Contact. Wear V. 249, I.7, pp 546-556, 2001. https://www.bib.irb.hr/73534

[8]- S. Saito, S. Yoneyama, and M. Takashi, 3-D Stress Analysis by Scattered Light photoelasticity, proceedings Volume 4317, Second International Conference on Experimental Mechanics; (2001). https://doi.org/10.1117/12.429560

[9]- G. Oppel : Untersuchung raumlicher Spannungs- und Dehnungszustande Forschunq 7.Bd./Heft 5,1936

[10]- R. Desailly et A. Lagard, sur une méthode de photoélasticité tridimensionnelle non destructive à champ complet, Journal de Mécanique Appliquée, Vol. n°1, pp. 3-30,1980.

[11]- J. Cernousek, Three-dimensional photoelasticity by Stress Freezing, Experimental Mechanics, pp.417-426, December 1980. https://citations.springer.com/item?doi=10.1007/BF02320882

[12]-] L. Kogut & I. Etsion, Elastic-Plastic contact analysis of a sphere and a rigid flat, Journal of Applied Mechanics, V. 69, pp.657 - 662,2002. DOI: 10.1115/1.1490373

[13]- A. Bilek, J.C. Dupré , A. Ouibrahim, F. Bremand, 3D Photoelasticity and numerical analysis of a cylinder/half-space contact problem, Computer Methods and Experimental Measurements for Surface Effects and Contact Mechanics VII, WIT Press Southampton, Boston 2005,pp. 173-182.

[14]- K.L. Johnson, Contact mechanics , Cambridge University press 1985

[15]-] J. A. Germaneau, F. Peyruseigt, S. Mistou, P. Doumalin and J.C. Dupré, Experimental study of stress repartition in aeronautical spherical plain bearing by 3D photoelasticity : validation of a numerical model, 5th BSSM International Conference on Advances in Experimental Mechanics, Sept. 2007, University of Manchester, UK.

[16]- Abodol Rasoul Sohouli, Ali Maozemi Goudarzi, Reza Akbari Alashti, Finite Element Analysis of Elastic-Plastic Contact Mechanic Considering the Effect of Contact Geometry and Material Propertie, Journal of Surface Engineered Materials and Advanced Technology, 2011, 1, 125-129. DOI: 10.4236/jsemat.2011.13019

[17]- T. L. Nguyen, A. Fatu, D. Souchet, Etude du contact entre le coussinet et le logement dans un palier lisse, 21ème Congrès Français de Mécanique, bordeaux 2013. https://docplayer.fr/9397165-Etude-du-contact-entre-le-coussinet-et-le-logement-dans-un-palier-lisse.html

[18]- Rabah Haciane, Ali Bilek, Said Larbi, Said Djebali, Photoelastic and numerical analysis of a sphere/plan contact problem, 1st International Conference on Structural Integrity, Procedia Engineering 114 (2015) 277 – 283. doi: 10.1016/j.proeng.2015.08.069

[19]- Karl-Hans Laermann, reflections on the Accuracy of photoelastic Stress Analysis (OIAZ), 142.Jg.,Hft.5/1997,396-401.

[20]- Tamraker and K. Ramesh, Simulation of error in digital photoelacticity by jones Calculus, Strain 2001 Vol.37 No.3.

[21]- S.J. Haake and E. A. Patterson, photoelastic Analysis of Frozen Stressed Specimen using Spectral Content Analysis. Experimental Mechanics, pp. 266-272, Sept 1992. https://doi.org/10.1007/BF02319365

[22]- A. Bilek & F. Djeddi, Photoelastic and numerical stress analysis of a 2D contact problem and 3D numerical solution for the case of a rigid body on a deformable one, Computational Methods and Experimental Measurements XV,

Editors G.M. Carlomagno & C.A. Brebbia WIT Press 2011, pp 167-177. ISSN 1743-355X**,** doi: 10.2495/CMEM110161

[23]- K. TOUAHIR, A. BILEK, S. LARBI and S. DJEBALI. The Birefringent Property of an Optical Resin for the Study of a Stress Field Developed in a Three Point Loading Beam , Premières Journées Internationales des Physique de Constantine Université Constantine 1,JIPC1,16-17 Décembre 2013. http://hdl.handle.net/123456789/135548.